Observational Study

Medicine®

OPEN

Screening and identification of key genes and pathways in metastatic uveal melanoma based on gene expression using bioinformatic analysis

Jialu Xie, MD[a], Zhenyu Wu, MD[a], Xiaogang Xu, PhD[b], Guanlu Liang, MD[a], Jiehui Xu, MD[a,*]

Abstract

The current study aimed to elucidate the molecular mechanisms and identify the potential key genes and pathways for metastatic uveal melanoma (UM) using bioinformatics analysis.

Gene expression microarray data from GSE39717 included 39 primary UM tissue samples and 2 metastatic UM tissue samples. Differentially expressed genes (DEGs) were generated using Gene Expression Omnibus 2R. Gene ontology (GO) and Kyoto Encyclopedia of Genes and Genomes (KEGG) pathway enrichment analyses were performed using the online Database for Annotation, Visualization and Integrated Discovery (DAVID) tool. The web-based STRING tool was adopted to construct a protein–protein interaction (PPI) network. The MCODE tool in Cytoscape was used to generate significant modules of the PPI network.

A total of 213 DEGs were identified. GO and KEGG analyses revealed that the upregulated genes were mainly enriched in extracellular matrix organization and blood coagulation cascades, while the downregulated DEGs were mainly related to protein binding, negative regulation of ERK cascade, nucleus and chromatin modification, and lung and renal cell carcinoma. The most significant module was extracted from the PPI network. GO and KEGG enrichment analyses of the module revealed that the genes were mainly enriched in the extracellular region and space organization, blood coagulation process, and PI3K-Akt signaling pathway. Hub genes, including *FN1, APOB, F2, SERPINC1, SERPINA1, APOA1, FGG, PROC, ITIH2, VCAN, TFPI, CXCL8, CDH2*, and *HP,* were identified from DEGs. Survival analysis and hierarchical clustering results revealed that most of the hub genes were associated with prognosis and clinical progression.

Results of this bioinformatics analysis may provide predictive biomarkers and potential candidate therapeutic targets for individuals with metastatic UM.

Abbreviations: DEGs = differentially expressed genes, DFS = disease-free survival, GO = Gene Ontology, GEO = Gene Expression Omnibus, KEGG = Kyoto Encyclopedia of Genes and Genomes, OS = overall survival, PPI = protein–protein interaction, UM = uveal melanoma.

Keywords: bioinformatics analysis, gene expression profiling, metastatic uveal melanoma

1. Introduction

Melanoma is a life-threatening malignancy and the primary intraocular form is known as uveal melanoma (UM). Among primary intraocular tumors in the adult population, UM is the most common. UM may originate from the choroid, iris, or ciliary body, which are commonly known as the uvea. In approximately 90% of UM cases, the choroid is involved.[1] The biological features and clinical behavior of UM are distinct from those of cutaneous melanoma. Currently, first-line treatment for UM includes resection, radiation, and eye enucleation. These therapy options are able to control the local disease but still did not reduce the risk of distant metastases, which is a key obstacle to improve the long-term survival of UM. Despite the emergence of novel treatment modalities, such as immune checkpoint blockade, gene-targeted therapy, and anti-angiogenic therapy, the survival rates of patients with UM have not changed in the past 40 years.[2]

Hematogenous metastases typically involve the liver in approximately 90% of metastatic cases, the lung(s) is involved in 24% of cases, and bone in 16%.[3,4] The median time from initial diagnosis to metastasis is approximately 2 to 3 years; once metastases occur, prognosis is typically poor, with a median survival of 2 to 3 months.[5,6] To improve the prognosis of metastatic UM, the mechanisms of how UM metastasizes and the

Editor: Abdul Rouf Banday.

The authors received no financial support for the research, authorship, and/or publication of this article.

The datasets generated during and/or analyzed during the current study are available from the corresponding author on reasonable request.

Supplemental Digital Content is available for this article.

The datasets generated during and/or analyzed during the current study are available from the corresponding author on reasonable request.

[a] Department of Ophthalmology, [b] Zhejiang Provincial Key Lab of Geriatrics & Geriatrics Institute of Zhejiang Province, Department of Geriatrics, Zhejiang Hospital, Hangzhou, China.

[*] Correspondence: Jiehui Xu, Department of Ophthalmology, Zhejiang Hospital, 12 Lingyin Road, Hanghzou 310013, Zhejiang Province, People's Republic of China (e-mail: zjhophthalmology@163.com)

How to cite this article: Xie J, Wu Z, Xu X, Liang G, Xu J. Screening and identification of key genes and pathways in metastatic uveal melanoma based on gene expression using bioinformatic analysis. Medicine 2020;99:43(e22974).

Received: 24 January 2020 / Received in final form: 5 September 2020 / Accepted: 28 September 2020

http://dx.doi.org/10.1097/MD.0000000000022974

prognostic factors that can predict the risk for metastasis have been extensively studied. Shields et al[7] reported that the thickness of UM is positively associated with increasing risk for metastasis. Schmittel et al[8] found that primary UMs with a largest diameter > 14 mm and ciliary body involvement have a poor prognosis. In addition, due to the advances in molecular biology, some researchers have found that noncoding RNAs,[9–11] aberrant alterations in chromosomes 1, 3, 6, and 8,[12–14] and loss-of-function mutations in the *BAP1* gene[15] are involved in metastasis. However, metastatic mechanisms in UM are particularly complicated, and there are no clinically applicable molecular biomarkers that can accurately predict metastatic risk.

In recent decades, advances in microarray technology and bioinformatics analysis have helped to identify key gene(s) and functional pathways involved in the progression and metastasis of cancers, which have offered new insights into the molecular mechanism of metastasis in UM. Thus, in the present study, messenger RNA (mRNA) microarray datasets from the Gene Expression Omnibus (GEO) database were obtained and analyzed to identify differentially expressed genes (DEGs) between patient-derived primary UM tissues and metastatic UM tissues, followed by Gene Ontology (GO), Kyoto Encyclopedia of Genes and Genomes (KEGG) pathway enrichment analysis. Subsequently, a protein–protein interaction (PPI) network was constructed to interpret the biological interaction of DEGs. Module analysis of the DEGs was performed to identify key genes and pathways related to metastatic UM. Finally, a total of 213 DEGs and 14 hub genes were identified, which may be potential prognostic markers and therapeutic targets for metastatic UM.

2. Materials and methods

2.1. Microarray data

The gene expression dataset GSE397127[16] was downloaded from the GEO database. The GEO (http://www.ncbi.nlm.nih.gov/geo)[17] is a public database of high-throughput gene expression data, chips, and microarrays. GSE397127 was based on the GPL6098 platform (Affymetrix Illumina humanRef-8 version 1.0 expression beadchip), which contained 39 primary UM tissue samples and 2 liver-metastatic UM samples. The probes were converted into official gene symbols according to the annotation information of the platform. The ethical approval was not necessary for this study, as all datasets were retrieved from a public database.

2.2. Identification of DEGs

GEO2R (https://www.ncbi.nlm.nih.gov/geo/geo2r/)[18] was used to screen DEGs between primary and metastatic UM tissue samples. GEO2R is an R-based application that enables users to identify DEGs in one or more datasets. LogFC (foldchange) > 3 and adj. A list of upregulated and downregulated DEGs were saved for subsequent analysis.

2.3. GO functional and KEGG pathway enrichment analyses

GO functional enrichment is a widely used approach for interpreting sets of genes.[19] The KEGG database is a collection of pathway maps representing metabolism and various other biological functions.[20] As a free online bioinformatics resource, the database for annotation, visualization, and integrated discovery (DAVID, https://david.ncifcrf.gov/) provides functional annotation and visualization of large-scale lists of genes.[21] In this study, DAVID was used for the enrichment of GO functions and KEGG pathways for the systematic analysis of DEGs. Differences with $P < .05$ were considered to be statistically significant.

2.4. PPI network of DEGs

The web-based STRING tool (https://string-db.org/) was adopted to obtain PPI relationships for the DEGs followed by visualization using Cytoscape. PPIs with a combined score > 0.4 were selected. Cytoscape is an open source software for integrating biomolecular interaction networks with high-throughput expression data into a unified conceptual framework.[22] The plug-in tool Molecular Complex Detection (MCODE) (version 1.5.1) of Cytoscape was adopted to detect strongly connected regions from the PPI network with the following parameters: degree cutoff = 2, k-core = 2, node score cutoff = 0.2, maximum depth = 100. MCODE is an application designed to find densely connected regions in a specific PPI network based on topology.[23]

2.5. Hub gene selection and analysis

Hub gene selection was performed using cytoHubba (version 0.1), a plug-in application of Cytoscape. CytoHubba computes 11 methods to identify important nodes in PPI networks.[24] Genes appearing at least twice in the top 10 results of each computation method were considered Hub genes. The analyses of clinical prognosis including overall survival (OS) and disease-free survival (DFS) of hub genes were performed using Kaplan–Meier curve analysis and analyzed using GEPIA online platform[25] (http://gepia.cancer-pku.cn/), and coexpression analysis of the hub genes were performed in both cBioPortal[26] and Oncomine databases (https://www.oncomine.org/).[27] Hierarchical clustering of hub genes was performed using the University of California Santa Cruz (UCSC) Xena platform (https://xenabrowser.net/).[28]

2.6. Statistical analysis

For identification of DEGs, the Student *t* test was adopted and Benjamini and Hochberg method was used to adjust the *P* value.[29] For KEGG and GO analyses, the Fisher exact test was performed to determine whether differences were significant. For the above statistical methodologies, *P* value less than .05 was considered statistically significant.

3. Results

3.1. Identification of DEGs

The microarray dataset GSE39717, deposited by Harbour et al,[16] was downloaded from the GEO database. A total of 24,358 genes from 39 primary UM and 2 metastatic UM patient-derived tumor tissues were obtained. A total of 213 DEGs were identified between the primary and metastatic samples, including 70 (32.9%) upregulated and 143 (67.1%) downregulated genes.

3.2. GO and KEGG enrichment analyses of DEGs

On the basis of the enrichment analysis of DEGs using DAVID, a total of 115 GO terms of upregulated genes and 34 GO terms of

Table 1

Top 5 GO functional enrichment analyses of upregulated and downregulated DEGs.

Category	Functional annotation ID	Description	Count	*P*
Upregulated				
CC	GO:0005576	extracellular region	41	1.61E-25
CC	GO:0005615	extracellular space	34	3.58E-20
CC	GO:0031012	extracellular matrix	19	1.62E-17
CC	GO:0072562	blood microparticle	13	2.95E-13
BP	GO:0030198	extracellular matrix organization	13	1.07E-11
Downregulated				
MF	GO:0005515	protein binding	87	.001522
CC	GO:0005634	nucleus	58	.002373
BP	GO:0070373	negative regulation of ERK1 and ERK2 cascade	4	.010049
BP	GO:0016569	covalent chromatin modification	5	.011246
MF	GO:0003682	chromatin binding	9	.0118

downregulated genes were obtained. GO analysis revealed that changes in upregulated DEGs were significantly associated with extracellular region, matrix organization, space, and blood microparticles, while the downregulated DEGs were mainly related to protein binding, nucleus, negative regulation of ERK1 and ERK2 cascade, and covalent chromatin modification chromatin binding (Table 1). As shown in the KEGG pathway enrichment analysis (Table 2), upregulated DEGs were mainly involved in complement and coagulation cascades, extracellular matrix (ECM)-receptor interaction, amebiasis, focal adhesion, and protein digestion and absorption. The pathways enriched in the downregulated DEGs were mainly nonsmall cell lung cancer and renal cell carcinoma.

3.3. PPI network construction and module analysis

The PPI network of DEGs was constructed using Cytoscape (Fig. 1) and the most significant module was obtained using the MCODE application. As shown in Figure 2, the most significant module (MCODE Score = 12.5) contained 25 nodes and 120 edges. GO and KEGG enrichment analyses of genes involved in this module were conducted using DAVID. GO term enrichment analysis revealed that the genes in the above module were mainly involved in extracellular region, extracellular space, endoplasmic reticulum lumen, ECM organization, blood microparticle, ECM structural constituents, platelet degranulation, collagen catabolic processes, and extracellular exosome (Table 3). The results of KEGG pathway enrichment revealed that the genes were mainly related to ECM-receptor interaction, focal adhesion, protein digestion and absorption, amebiasis, PI3K-Akt signaling pathway, complement and coagulation cascades, platelet activation, small cell lung cancer, vitamin digestion and absorption, and proteoglycans in cancer (Table 4).

3.4. Hub gene selection and analysis

A total of 14 genes were identified as hub genes from 33 candidate genes using the cytoHubba tool in Cytoscape (Supplemental Digital Content [Table S1, http://links.lww.com/MD/F114]). The gene symbol, full name, and brief introduction of the functions for these hub genes are listed in Table 5. As illustrated in Figure 3, the survival analysis of the hub genes was performed using Kaplan–Meier curve analysis. In the OS analysis, the UM patients with high mRNA levels of *FN1, VCAN, APOA1*, and *PROC* genes demonstrated a worse prognosis (Fig. 3A). Meanwhile, UM patients with high mRNA levels of *FN1, VCAN, SERPINC1*, and *ITIH2* demonstrated worse DFS (Fig. 3B). According to the results of cytoHubba analysis, *FN1, APOB, F2, SERPINC1,* and *FGG* were ranked highest, which suggested their potential role in UM metastasis. The prognosis analysis results indicated that the alteration of *FN1* and *VCAN* mRNA levels was associated with worse OS and DFS. Nevertheless, APOPA1 and PROC worsen the OS while *SERPINC1* and *ITIH2* reduced DFS, although no statistical significance of the reduction was observed in OS affected by *APOA1* and the reduction of DFS affected by *FN1, SERPINC1,* and *ITIH2*. Furthermore, hierarchical clustering analysis the UCSC Xena platform revealed that the mRNA levels of *FN1, SERPINC1, SERPINA1, VCAN, PROC,* and *CDH2* were basically consistent with clinical grade (Fig. 4). Coexpression analysis using cBioPortal revealed that *FN1* genes were highly coexpressed with VCAN in the UM tissue (Pearson correlation, 0.70; Spearman correlation, 0.85) (Fig. 5A). The

Table 2

Top enriched KEGG pathways of upregulated and downregulated DEGs.

Category	Functional annotation ID	Description	Count	*P*
Upregulated				
KEGG	hsa04610	Complement and coagulation cascades	9	6.09E-09
KEGG	hsa04512	ECM-receptor interaction	9	3.93E-08
KEGG	hsa05146	Amoebiasis	9	1.86E-07
KEGG	hsa04510	Focal adhesion	11	2.97E-07
KEGG	hsa04974	Protein digestion and absorption	6	1.79E-04
Downregulated				
KEGG	hsa05223	Non-small cell lung cancer	3	.057856
KEGG	hsa05211	Renal cell carcinoma	3	.077159

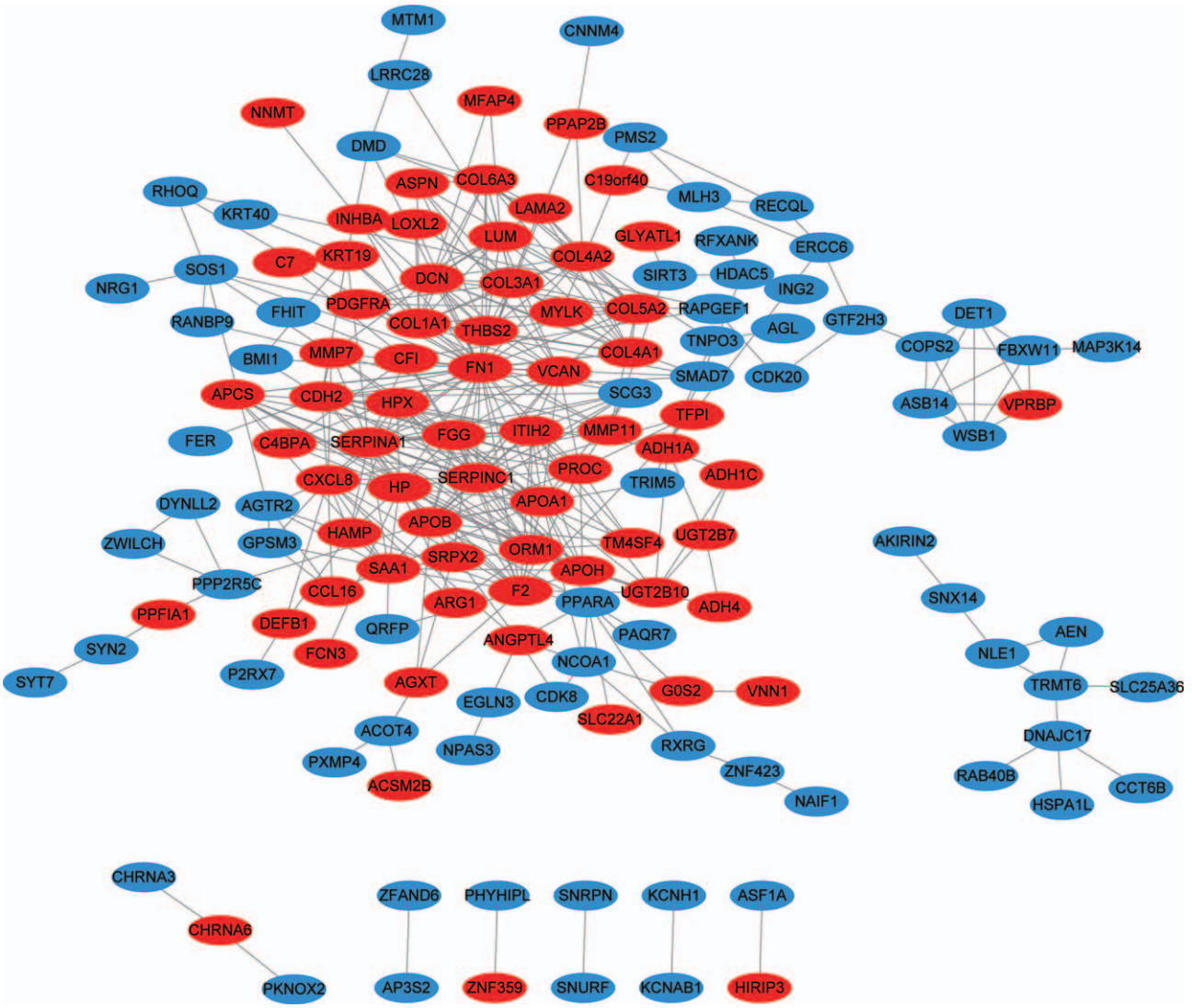

Figure 1. PPI network of DEGs was constructed using STRING and visualized in Cytoscape. Upregulated genes are marked in red; downregulated genes are marked in blue.

Laurent Melanoma data in Oncomine revealed that the expression of *VCAN* was positively related to *FN1* in 3 subtypes of UM (correlation index, 0.603) (Fig. 5B).

4. Discussion

UM is one of the most common intraocular malignancies in adults; 62% of UM patients have confirmed melanoma metastasis at the time of death and 92% of metastatic sites are the liver.[4] Currently, the management of liver metastasis from UM includes surgery, local chemotherapy, radiotherapy, and immune-embolization. Nevertheless, treatment of metastatic UM remains a daunting challenge in clinical practice due to the very poor prognosis of these patients.[30] Benefitting from updated prognostication techniques, primary UM can be classified into distinct subgroups with various levels of metastatic risk based on gene expression profile.[31] In 2004, Onken et al[32] proposed that mRNA levels of *PHLDA1*, *FZD6*, and *ENPP2* could be used as molecular signatures to predict prognosis. However, the oncogenic and metastatic mechanisms of UM remain controversial, and advances in the treatment of UM are not promising because survival of patients with UM has remained unchanged over the past 4 decades, from 1973 to 2013.[33] Hence, identification of key genes and pathways of the metastatic mechanism of UM could contribute to the diagnosis and treatment of UM.

In the present study, gene expression profiles of 39 primary UM samples and 2 metastatic UM samples were obtained from the GEO39717 dataset. A total of 213 DEGs were identified, including 70 upregulated and 143 downregulated genes. To further understand the interactions of the DEGs, GO function and KEGG pathway analyses were performed using DAVID. The upregulated genes were mainly enriched in extracellular region, matrix organization, space and blood microparticle, complement and coagulation cascades, ECM-receptor interaction, amebiasis, focal adhesion and protein digestion and absorption, while the downregulated DEGs were mainly related to protein binding, nucleus, negative regulation of ERK1 and ERK2 cascade, covalent chromatin modification chromatin binding, nonsmall cell lung cancer, and renal cell carcinoma. In the most significant module generated by MCODE, DEGs were mainly enriched in

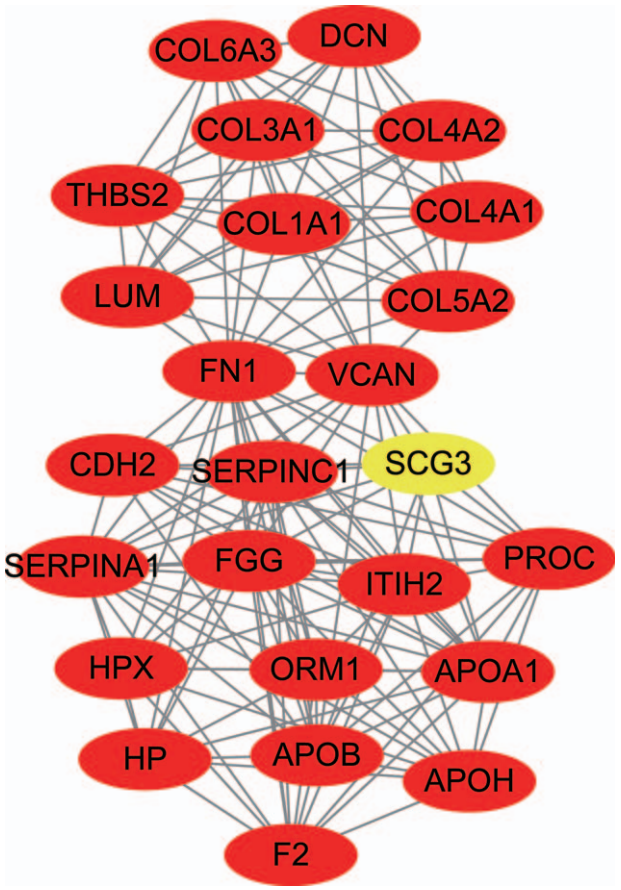

Figure 2. The most significant module of DEGs. The most significant module containing 25 nodes and 120 edges was extracted from PPI network using MCODE. Seed node was marked in yellow.

extracellular region and space organization, blood coagulation process and the PI3K-Akt signaling pathway. According to previous studies, the extracellular environment is the key driver for both cancer development and progression.[34] Blood coagulation pathways play a role in tumor progression and metastasis,[35–37] phosphor-AKT protein levels are positively associated with a higher risk for metastasis in patients with UM,[26] and ERK pathway promotes carcinogenesis and maintenance of UM.[38] Thus, results of all of these studies support those of the current investigation.

Hub genes, namely *FN1, APOB, F2, SERPINC1, SERPINA1, APOA1, FGG, PROC, ITIH2, VCAN, TFPI, CXCL8, CDH2*, and *HP*, were identified from the PPI network of DEGs using the cytoHubba tool, indicating these genes may be vital in the metastatic process of UM. *FN1* is involved in cell adhesion, cell motility, wound healing, and maintenance of cell shape. *FN1* has been shown to promote metastasis in various types of tumors.[39–41] Recently, Li et al[42] reported that *FN1* promotes cutaneous melanoma proliferation and metastasis by inhibiting apoptosis and regulating epithelial-to-mesenchymal transition, which is consistent with our results. APOA1 is the main protein constituent of high-density lipoprotein, which shuttles excess cholesterol from organs to the liver for excretion. APOA1 has been described to exert anti-apoptotic, anti-inflammatory, and antioxidant activities, which are involved in tumorigenesis.[43] In a murine model of malignant melanoma, APOA1 also demonstrated anti-tumor effects.[44] However, in the present study, we determined that APOA1 significantly increased in liver metastatic UM samples, indicating a stimulating role of APOA1 in UM metastasis. However, we cannot exclude the possibility that the increased APOA1 mRNA in liver metastatic UM was due to the fact that APOA1 mRNA levels are higher in the liver than any other tissue in the human body.[45] APOB is a major protein constituent of chylomicrons, low-density lipoprotein and very-low density lipoprotein, lung cancer and colorectal cancer risk were increased with high APOB levels,[46] whereas the role of APOB in UM remains unclear. SERPINA1 and SERPINC1 are members of the serpin family, SERPINA1 was found to improve nonsmall cell lung cancer cell migration, colony formation, and resistance to apoptosis,[47] while knockdown of SERPINC1 was reported to inhibit neural progenitor cell proliferation via suppression of the PI3K/Akt/mTOR signaling pathway.[48] ITIH2, also known as serum-derived HA-associated protein (SHAP), forms complexes with hyaluronan (HA) to regulate the localization, synthesis, and degradation of HA in serum. Elevated serum levels of the SHAP-HA complex indicate poor prognosis in endometrial and ovarian cancers.[49,50] VCAN plays a role in intercellular signaling and in connecting cells with the ECM. It was reported that VCAN significantly increased in superficial spreading melanoma tissue and metastatic melanoma cell lines.[51,52] Notably, another interesting finding of hub genes was that VCAN is highly relevant to FN1. Soikkeli et al[53] reported that in melanoma lymph nodes, upregulation of *POSTN, FN1, COL-I*, and *VCAN* genes was confirmed in metastatic outgrowth, and all of these genes were inducible by transforming growth factor-beta, which indicated the activation

Table 3

Top 10 GO functional enrichment analyses in the most significant DEG module.

Category	Functional annotation ID	Description	Count	*P*
CC	GO:0005576	extracellular region	24	1.10E-23
CC	GO:0005615	extracellular space	18	1.12E-14
CC	GO:0005788	endoplasmic reticulum lumen	11	2.30E-14
CC	GO:0031012	extracellular matrix	12	3.57E-14
BP	GO:0030198	extracellular matrix organization	11	6.34E-14
CC	GO:0072562	blood microparticle	9	1.28E-11
MF	GO:0005201	extracellular matrix structural constituent	7	3.96E-10
BP	GO:0002576	platelet degranulation	7	5.66E-09
BP	GO:0030574	collagen catabolic process	6	2.76E-08
CC	GO:0070062	extracellular exosome	16	2.09E-07

Table 4

Top 10 KEGG pathway enrichment analyses in the most significant DEG module.

Category	Functional annotation ID	Description	Count	*P*
KEGG	hsa04512	ECM-receptor interaction	8	1.15E-09
KEGG	hsa04510	Focal adhesion	8	4.69E-07
KEGG	hsa04974	Protein digestion and absorption	6	2.30E-06
KEGG	hsa05146	Amoebiasis	6	5.77E-06
KEGG	hsa04151	PI3K-Akt signaling pathway	8	1.48E-05
KEGG	hsa04610	Complement and coagulation cascades	5	2.55E-05
KEGG	hsa04611	Platelet activation	4	.004372
KEGG	hsa05222	Small cell lung cancer	3	.020307
KEGG	hsa04977	Vitamin digestion and absorption	2	.056095
KEGG	hsa05205	Proteoglycans in cancer	3	.094918

of the transforming growth factor-beta signaling pathway. Although FN1 and VCAN have been found to be positively associated with UM metastasis, the downstream protein and concrete mechanism of VCAN, as well as the interaction of FN1 and VCAN, remains unclear. *TFPI* encodes a serine protease inhibitor that regulates the tissue factor dependent pathway of blood coagulation. TPFI contributes to the development of multiple drug resistance in breast cancer cells.[54,55] CXCL8, also known as interleukin-8, is a member of the CXC chemokine family and is a mediator of the inflammatory response by regulating cancer stem cell proliferation and self-renewal, the CXCL8-CXCR1/2 axis may play an important role in tumor progression and metastasis.[56] In melanoma, NFAT1 regulates CXCL-8/MMP3 and promotes tumor growth and lung metastasis.[57] CDH2, also known as N-cadherin, belongs to the cadherin superfamily, and mediates calcium-dependent cell-cell adhesion. Elevated CDH2 is a well-known protein marker for the onset of epithelial-mesenchymal transition, which results in enhanced migratory capacity, invasiveness, and increased resistance to apoptosis in many types of cancers.[58] In melanoma cells, increased N-cadherin expression contributes to proliferation and invasive potential by activating PI3/AKT, mTOR, and ERK kinase.[59] The *HP* gene encodes haptoglobin, which combines with free plasma hemoglobin, thus enabling heme iron to be recycled in hepatocytes. Previous research found that cellular levels of HP are strongly associated with the recurrence rate of human head and neck cancers.[60] A positive correlation between elevated serum haptoglobin level and the incidence of colorectal cancer was also observed.[61]

In addition, we performed hierarchical clustering and prognosis analysis for hub genes. The hierarchical clustering results illustrated that, as the clinical stage of UM increased, most of the hub gene mRNA levels also increased, indicating the consistency between hub gene expression and UM tumor progression. In addition, OS and DFS analysis of the hub genes demonstrated that high expression of FN1 and VCAN was related to worse OS and DFS, increased APOA1 and PROC reduced OS, while SERPINC1 and ITIH2 reduced DFS. Analysis of hub genes demonstrated that these genes may play an important role(s) in the progression, invasion, and metastasis of UM, and may be potential candidates for prognosis prediction and diagnostic biomarkers.

Finally, there were several limitations to the current study. First, all of the data were obtained from the GEO database rather than directly from UM patient tissues. Second, all conclusions were based on bioinformatics analysis; hence, caution must be

Table 5

Full name and functional roles of 14 hub genes.

No.	Gene symbol	Full name	Function
1	FN1	Fibronectin 1	Fibronectins bind cell surfaces and various compounds, including collagen, fibrin, and DNA
2	APOB	Apolipoprotein B	APOB is a major protein constituent of chylomicrons, LDL, and VLDL
3	F2	Coagulation factor II, Thrombin	F2 is cleaved to form thrombin in the first step of the coagulation cascade, which results in the stemming of blood loss
4	SERPINC1	Serpin Family C Member 1	SERPINC1 is a plasma protease inhibitor and a member of the serpin superfamily
5	FGG	Fibrinogen Gamma Chain	FGG polymerizes to form an insoluble fibrin matrix together with FGA and FGB
6	SERPINA1	Serpin Family A Member 1	SERPINA1 is an inhibitor of serine proteases whose primary target is elastase
7	APOA1	Apolipoprotein A1	APOA1 is the major protein component of HDL in plasma
8	PROC	Protein C, Inactivator of Coagulation Factors Va and VIIIa	PROC is a vitamin K-dependent serine protease that regulates blood coagulation
9	ITIH2	Inter-Alpha-Trypsin Inhibitor Heavy Chain 2	ITIH2 may act as a carrier of hyaluronan in serum or as a binding protein between hyaluronan and other matrix protein
10	VCAN	Versican	VCAN may play a role in intercellular signaling and in connecting cells with the extracellular matrix
11	TFPI	Tissue factor pathway inhibitor	TFPI encodes a Kunitz-type serine protease inhibitor that regulates the tissue factor (TF)-dependent pathway of blood coagulation
12	CXCL8	C-X-C Motif Chemokine Ligand 8	CXCL8 is a member of the CXC chemokine family and is a major mediator of the inflammatory response
13	CDH2	Cadherin 2	CDH2 preferentially mediates homotypic cell-cell adhesion by dimerization with a CDH2 chain from another cell
14	HP	Haptoglobin	HP combines with free plasma hemoglobin to allow hepatic recycling of hemeiron and to prevent kidney damage

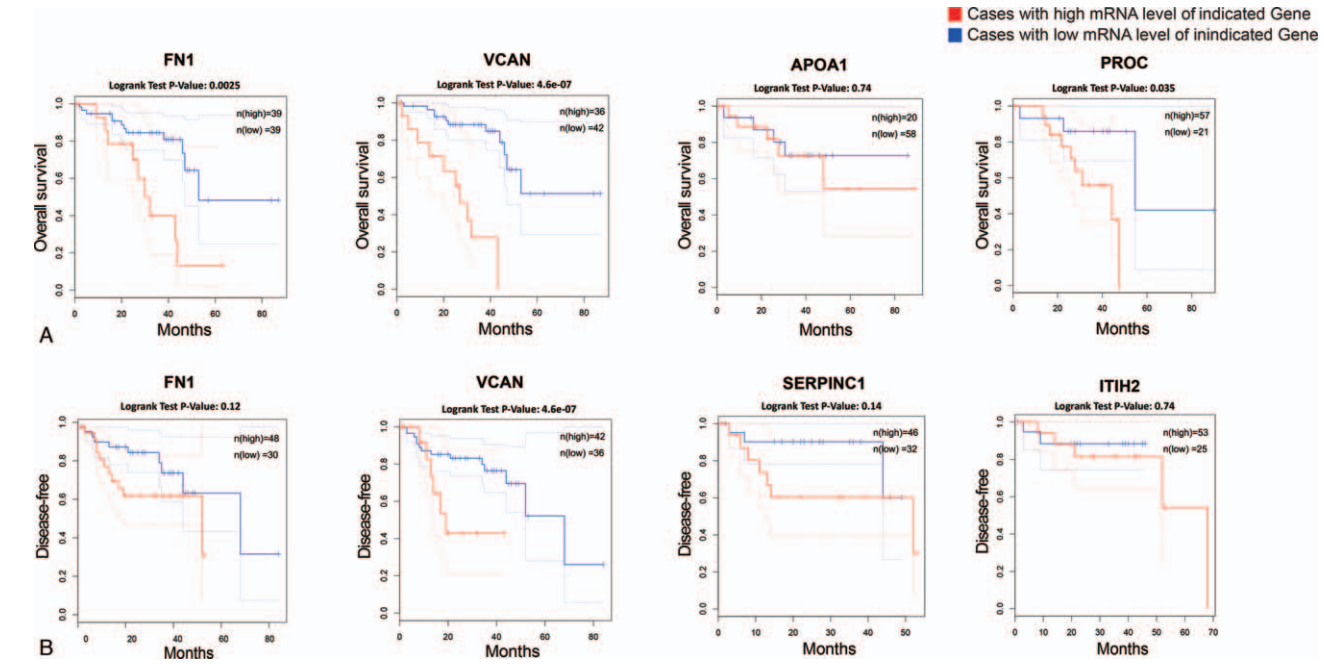

Figure 3. (A) Overall survival and (B) disease-free survival analyses of hub genes were performed using GEPIA platform.

exercised in interpreting the results, being aware that experimental verification is a better approach to confirm findings. Third, the GSE 39717 dataset consisted of 39 primary tumor samples and 2 metastatic samples, the imbalance between groups may have unintentionally introduced biases. In summary, larger-scale tissue samples derived from a primary and metastatic UM patient cohort with confirmatory experiments need to be performed to verify our conclusions.

5. Conclusion

The present bioinformatic analysis identified key genes and molecular pathways possibly involved in the metastatic process of UM. A total of 213 DEGs and 14 hub genes were identified to play crucial roles in the progression, invasion, and metastasis of UM, and could be potential candidates as diagnostic biomarkers.

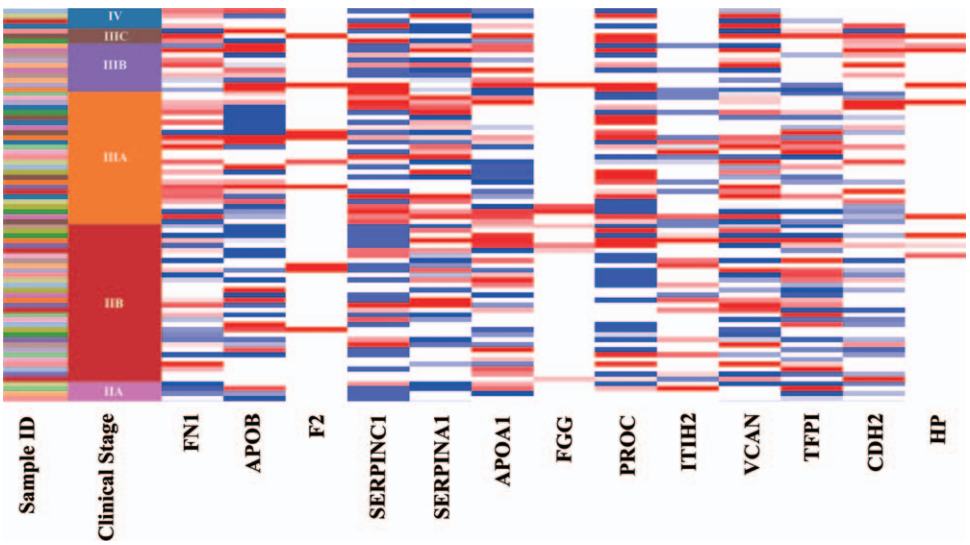

Figure 4. Hierarchical clustering of hub genes was performed using UCSC Xena platform. Upregulation of gene is marked in red, downregulation of genes is marked in blue.

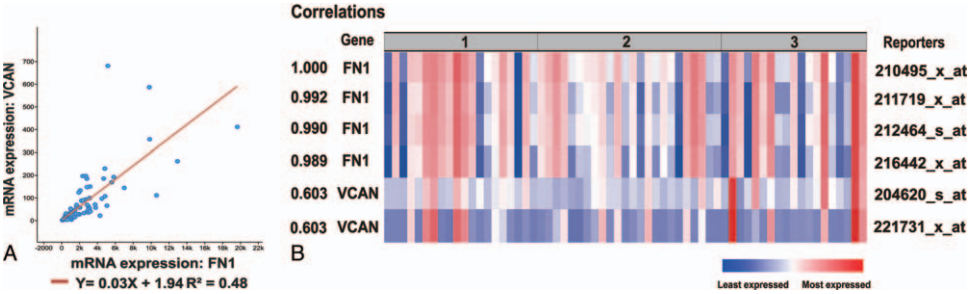

Figure 5. FN1 and VCAN expression directly correlates in human uveal melanoma cancers. (A) Coexpression analysis of FN1 and VCAN via cBioPortal platform. (B) FN1 gene coexpressed with FN1 in Laurent Melanoma data in Oncomine database, which consists of three subtypes: 1. Epitheliod Cell Uveal Melanoma 2. Mixed Cell Uveal Melanoma 3. Uveal Melanoma. The reporters indicate probes used in the analysis. Upregulation of expression is marked in red and downregulation is blue, passing by white, with fluctuating color intensity.

Acknowledgments

We thank Wolters Kluwer for English language editing.

Author contributions

Conceptualization: Jiehui Xu, Jialu Xie.
Formal analysis: Zhenyu Wu.
Investigation: Jiehui Xu.
Project administration: Jiehui Xu.
Data curation: Jialu Xie, Xiaogang Xu.
Methodology: Jialu Xie, Zhenyu Wu.
Visualization: Jialu Xie.
Writing – original draft: Jialu Xie, Guanlu Liang.
Writing – review & editing: Jialu Xie, Xiaogang Xu.

Correction

When originally published, Dr. Xiagang Xu's degree appeared incorrectly as MD. It has been corrected to PhD.

References

[1] Wu MY, Lai TT, Liao WT, et al. Clinicopathological and prognostic significance and molecular mechanisms governing uveal melanoma. Ther Adv Med Oncol 2020;12:1758835920917566.
[2] Grisanti S, Tura A. Uveal melanoma Exon Publications 2018;1–8.
[3] Grossniklaus HE. Understanding uveal melanoma metastasis to the liver: the Zimmerman effect and the Zimmerman hypothesis. Ophthalmology 2019;126:483–7.
[4] Assessment of metastatic disease status at death in 435 patients with large choroidal melanoma in the Collaborative Ocular Melanoma Study (COMS): COMS report no. 15. Arch Ophthalmol 2001; 119:670–676.
[5] Lane AM, Kim IK, Gragoudas ES. Survival rates in patients after treatment for metastasis from uveal melanoma. JAMA Ophthalmol 2018;136:981–6.
[6] Gragoudas ES, Egan KM, Seddon JM, et al. Survival of patients with metastases from uveal melanoma. Ophthalmology 1991;98:383–9. discussion 90.
[7] Shields CL, Furuta M, Thangappan A, et al. Metastasis of uveal melanoma millimeter-by-millimeter in 8033 consecutive eyes. Arch Ophthalmol 2009;127:989–98.
[8] Schmittel A, Bechrakis NE, Martus P, et al. Independent prognostic factors for distant metastases and survival in patients with primary uveal melanoma. Eur J Cancer 2004;40:2389–95.
[9] Larsen AC, Holst L, Kaczkowski B, et al. MicroRNA expression analysis and Multiplex ligation-dependent probe amplification in metastatic and non-metastatic uveal melanoma. Acta Ophthalmol 2014;92:541–9.
[10] Sun L, Bian G, Meng Z, et al. MiR-144 inhibits uveal melanoma cell proliferation and invasion by regulating c-Met expression. PLoS One 2015;10:e0124428.
[11] Sun L, Sun P, Zhou QY, et al. Long noncoding RNA MALAT1 promotes uveal melanoma cell growth and invasion by silencing of miR-140. Am J Transl Res 2016;8:3939–46.
[12] Horsman DE, Sroka H, Rootman J, et al. Monosomy 3 and isochromosome 8q in a uveal melanoma. Cancer Genet Cytogenet 1990;45:249–53.
[13] Tschentscher F, Prescher G, Zeschnigk M, et al. Identification of chromosomes 3, 6, and 8 aberrations in uveal melanoma by microsatellite analysis in comparison to comparative genomic hybridization. Cancer Genet Cytogenet 2000;122:13–7.
[14] Prescher G, Bornfeld N, Becher R. Nonrandom chromosomal abnormalities in primary uveal melanoma. J Natl Cancer Inst 1990;82:1765–9.
[15] Harbour JW, Onken MD, Roberson ED, et al. Frequent mutation of BAP1 in metastasizing uveal melanomas. Science 2010;330:1410–3.
[16] Harbour JW, Roberson EDO, Anbunathan H, et al. Recurrent mutations at codon 625 of the splicing factor SF3B1 in uveal melanoma. Nat Genet 2013;45:133–5.
[17] Edgar R, Domrachev M, Lash AE. Gene expression omnibus: NCBI gene expression and hybridization array data repository. Nucleic Acids Res 2002;30:207–10.
[18] Barrett T, Wilhite SE, Ledoux P, et al. NCBI GEO: archive for functional genomics data sets—update. Nucleic Acids Research 2012;41:D991–5.
[19] Consortium GO. The Gene Ontology (GO) project in 2006. Nucleic Acids Res 2006;34:D322–6.
[20] Kanehisa M, Goto S. KEGG: kyoto encyclopedia of genes and genomes. Nucleic Acids Res 2000;28:27–30.
[21] Huang da W, Sherman BT, Lempicki RA. Systematic and integrative analysis of large gene lists using DAVID bioinformatics resources. Nat Protoc 2009;4:44–57.
[22] Shannon P, Markiel A, Ozier O, et al. Cytoscape: a software environment for integrated models of biomolecular interaction networks. Genome Res 2003;13:2498–504.
[23] Bandettini WP, Kellman P, Mancini C, et al. MultiContrast Delayed Enhancement (MCODE) improves detection of subendocardial myocardial infarction by late gadolinium enhancement cardiovascular magnetic resonance: a clinical validation study. J Cardiovasc Magn Reson 2012;14:83.
[24] Chin CH, Chen SH, Wu HH, et al. cytoHubba: identifying hub objects and sub-networks from complex interactome. BMC Syst Biol 2014;Suppl 4:S11.
[25] Tang Z, Li C, Kang B, et al. GEPIA: a web server for cancer and normal gene expression profiling and interactive analyses. Nucleic Acids Res 2017;45:W98–w102.
[26] Cerami E, Gao J, Dogrusoz U, et al. The cBio cancer genomics portal: an open platform for exploring multidimensional cancer genomics data. Cancer Discov 2012;2:401–4.
[27] Rhodes DR, Yu J, Shanker K, et al. ONCOMINE: a cancer microarray database and integrated data-mining platform. Neoplasia 2004; 6:1–6.
[28] Goldman M, Craft B, Hastie M, et al. The UCSC Xena platform for public and private cancer genomics data visualization and interpretation. bioRxiv 2019;326470.
[29] Benjamini Y, Hochberg Y. Controlling the false discovery rate: a practical and powerful approach to multiple testing. J Royal Stat Soc Series B (Methodological) 1995;57:289–300.

[30] Rowcroft A, Loveday BPT, Thomson BNJ, et al. Systematic review of liver directed therapy for uveal melanoma hepatic metastases. HPB (Oxford) 2019.
[31] Werdich XQ, Jakobiec FA, Singh AD, et al. A review of advanced genetic testing for clinical prognostication in uveal melanoma. Semin Ophthalmol 2013;28:361–71.
[32] Onken MD, Worley LA, Ehlers JP, et al. Gene expression profiling in uveal melanoma reveals two molecular classes and predicts metastatic death. Cancer Res 2004;64:7205–9.
[33] Aronow ME, Topham AK, Singh AD. Uveal melanoma: 5-year update on incidence, treatment, and survival (SEER 1973-2013). Ocul Oncol Pathol 2018;4:145–51.
[34] Walker C, Mojares E, Del Rio Hernandez A. Role of extracellular matrix in development and cancer progression. Int J Mol Sci 2018;19:
[35] Guglietta S, Rescigno M. Hypercoagulation and complement: connected players in tumor development and metastases. Semin Immunol 2016; 28:578–86.
[36] Unlu B, Versteeg HH. Effects of tumor-expressed coagulation factors on cancer progression and venous thrombosis: is there a key factor? Thromb Res 2014;133(suppl 2):S76–84.
[37] Falanga A, Marchetti M, Vignoli A. Coagulation and cancer: biological and clinical aspects. J Thromb Haemost 2013;11:223–33.
[38] Li Y, Yu P, Zou Y, et al. KRas-ERK signalling promotes the onset and maintenance of uveal melanoma through regulating JMJD6-mediated H2A.X phosphorylation at tyrosine 39. Artif Cells Nanomed Biotechnol 2019;47:4257–65.
[39] Yoshihara M, Kajiyama H, Yokoi A, et al. Ovarian cancer-associated mesothelial cells induce acquired platinum-resistance in peritoneal metastasis via the FN1/Akt signaling pathway. Int J Cancer 2020.
[40] Cai X, Liu C, Zhang TN, et al. Down-regulation of FN1 inhibits colorectal carcinogenesis by suppressing proliferation, migration, and invasion. J Cell Biochem 2018;119:4717–28.
[41] Wang S, Gao B, Yang H, et al. MicroRNA-432 is downregulated in cervical cancer and directly targets FN1 to inhibit cell proliferation and invasion. Oncol Lett 2019;18:1475–82.
[42] Li B, Shen W, Peng H, et al. Fibronectin 1 promotes melanoma proliferation and metastasis by inhibiting apoptosis and regulating EMT. Onco Targets Ther 2019;12:3207–21.
[43] Zamanian-Daryoush M, DiDonato JA. Apolipoprotein A-I and cancer. Front Pharmacol 2015;6:265.
[44] Zamanian-Daryoush M, Lindner D, Tallant TC, et al. The cardioprotective protein apolipoprotein A1 promotes potent anti-tumorigenic effects. J Biol Chem 2013;288:21237–52.
[45] Uhlen M, Fagerberg L, Hallstrom BM, et al. Proteomics. Tissue-based map of the human proteome. Science 2015;347:1260419.
[46] Borgquist S, Butt T, Almgren P, et al. Apolipoproteins, lipids and risk of cancer. Int J Cancer 2016;138:2648–56.
[47] Ercetin E, Richtmann S, Delgado BM, et al. Clinical significance of SERPINA1 gene and its encoded alpha1-antitrypsin protein in NSCLC. Cancers (Basel) 2019;11:
[48] Xu J, Ying Y, Xiong G, et al. Knockdown of serpin peptidase inhibitor clade C member 1 inhibits the growth of nasopharyngeal carcinoma cells. Mol Med Rep 2019;19:3658–66.
[49] Yabushita H, Iwasaki K, Kanyama K, et al. Clinicopathological role of serum-derived hyaluronan-associated protein (SHAP)-hyaluronan complex in endometrial cancer. Obstet Gynecol Int 2011;2011: 739150.
[50] Obayashi Y, Yabushita H, Kanyama K, et al. Role of serum-derived hyaluronan-associated protein-hyaluronan complex in ovarian cancer. Oncol Rep 2008;19:1245–51.
[51] Jeffs AR, Glover AC, Slobbe LJ, et al. A gene expression signature of invasive potential in metastatic melanoma cells. PLoS One 2009;4: e8461.
[52] Gambichler T, Kreuter A, Grothe S, et al. Versican overexpression in cutaneous malignant melanoma. Eur J Med Res 2008;13:500–4.
[53] Soikkeli J, Podlasz P, Yin M, et al. Metastatic outgrowth encompasses COL-I, FN1, and POSTN up-regulation and assembly to fibrillar networks regulating cell adhesion, migration, and growth. Am J Pathol 2010;177:387–403.
[54] Arnason T, Harkness T. Development, maintenance, and reversal of multiple drug resistance: at the crossroads of TFPI1, ABC transporters, and HIF1. Cancers (Basel) 2015;7:2063–82.
[55] Davies GF, Berg A, Postnikoff SD, et al. TFPI1 mediates resistance to doxorubicin in breast cancer cells by inducing a hypoxic-like response. PLoS One 2014;9:e84611.
[56] Ha H, Debnath B, Neamati N. Role of the CXCL8-CXCR1/2 axis in cancer and inflammatory diseases. Theranostics 2017;7:1543–88.
[57] Shoshan E, Braeuer RR, Kamiya T, et al. NFAT1 directly regulates IL8 and MMP3 to promote melanoma tumor growth and metastasis. Cancer Res 2016;76:3145–55.
[58] Kalluri R, Weinberg RA. The basics of epithelial-mesenchymal transition. J Clin Invest 2009;119:1420–8.
[59] Ciolczyk-Wierzbicka D, Laidler P. The inhibition of invasion of human melanoma cells through N-cadherin knock-down. Med Oncol 2018; 35:42.
[60] Li SC, Lee CC, Hsu CM, et al. IL-6 induces haptoglobin expression through activating STAT3 in human head and neck cancer. J Oral Pathol Med 2020;49:49–54.
[61] Ghuman S, Van Hemelrijck M, Garmo H, et al. Serum inflammatory markers and colorectal cancer risk and survival. Br J Cancer 2017; 116:1358–65.